Raman and Infrared Spectra of Thymine. A Matrix Isolation and DFT Study†

Krystyna Szczepaniak,* M. Martin Szczesniak,‡ and Willis B. Person*

Department of Chemistry, P.O. Box 117200, University of Florida, Gainesville, Florida 32611

Received: December 15, 1999; In Final Form: February 16, 2000

The Raman spectrum has been measured for thymine isolated in an Ar matrix using an FTRA instrument with infrared excitation at 1.064 μm, thereby avoiding complications due to resonance Raman and fluorescence effects. This spectrum is used, together with the newly measured infrared spectrum, to establish the assignment of the vibrational spectra of isolated thymine. The assignment is assisted by DFT calculations made at the B3LYP/6-31G(d,p) level of theory, using GAUSSIAN 98W. The calculated spectra, including the Raman spectrum, are in surprisingly good agreement with the experimental spectra. The discrepancies that are observed for some parts of the spectrum result primarily from the failure of the harmonic approximation made in the calculation. The effect of the neglect of anharmonicity has been investigated by determining a set of effective force constants that reproduce the experimental frequencies and intensity patterns in the infrared and Raman spectra and by examining how the predicted spectra (intensities, frequencies, potential energy distributions (PEDs), infrared intensity distributions (IDs), and Raman intensity distributions (RIDs)) change. The final results provide an unambiguous assignment of the vibrational spectra for thymine isolated in an Ar matrix and illustrate that the concepts of PEDs, IDs, and RIDs are useful for the interpretation of the vibrational spectra of molecules the size of the pyrimidine bases. Comparison of the Raman spectrum of thymine isolated in the Ar matrix with that of a polycrystalline sample indicates that they are quite similar, in marked contrast to the differences in the corresponding infrared spectra.

Introduction

Infrared (IR) and Raman (RA) spectroscopy are powerful tools for the study of force fields and conformations of nucleic acids and their components. However, the correlation between structure, force fields, and vibrational spectra is by no means straightforward for molecules as large as the pyrimidine and purine bases. In principle, this correlation may be found by combining a reliable quantum-mechanical calculation of the vibrational spectra with experimental studies of these spectra, but relating the calculated spectrum to the experimental spectrum involves many problems because of the anharmonic nature of the latter (anharmonicity corrections and Fermi resonance, to name just two).

To use the calculated vibrational spectra as a source of information concerning the structure and force field of the nucleic-acid bases, it is essential to test the calculation by comparing the calculated with the experimental spectrum of the molecule under the same condition. If the calculation is for the molecule in vacuo, the experimental spectrum should also be measured for *isolated* molecules. At present, such experimental spectra can be obtained relatively easily by trapping molecules in an inert solid argon environment, in which they have properties very similar to those in the vapor.[1,2] The experimental spectrum of such isolated molecules may be obtained over a wide spectral region because there is no interfering IR and RA absorption from the argon matrix. The matrix isolation technique for pyrimidine or purine bases also avoids the complications arising from the decomposition of the sample during spectroscopic studies of the vapor phase, which require quite elevated temperatures to achieve vapor pressures high enough to be able to observe the weaker spectral features.

During the past decade, IR spectra of nucleic-acid bases (including thymine, as well as many modified analogues) isolated in an argon matrix have been investigated[2−5] (and the references therein). This is not the case for their Raman spectra. To our knowledge, this work is only the second study of the RA spectrum of a matrix-isolated nucleic-acid base, after the pioneering work on uracil in 1984 by Barnes et al.[5] However, many studies have been made of the RA spectra of nucleic-acid bases in solution or in solid state, and the results have been used in the elucidation of the structure and conformation of nucleic acids. The RA spectra of these solids (or solutions) were interpreted using results from quantum-mechanical calculations made for an isolated molecule. In the particular case of solid thymine, we cite the three most recent reports from the laboratories of Tsuboi,[6,7] Peticolas,[8] and Berthier,[9] which also refer to the history of such study.

In this report, we shall present and analyze the Fourier transform RA (FTRA) spectrum (nonresonance) of thymine isolated in an argon matrix and compare this spectrum with the IR (FTIR) spectrum of isolated thymine. Although the IR spectrum of matrix-isolated thymine has been thoroughly studied before,[10−12] we have at least two reasons for reexamining this spectrum here: (1) we have used a more sensitive FTIR spectrometer, which allowed the study of very dilute matrices, providing much better-resolved spectra with very little aggregation; and (2) it is important to compare all of the details of both IR and RA spectra for matrix-isolated thymine plotted and analyzed together to obtain as much information for their interpretation as possible.

The quantum mechanical results we utilize for our interpretation of the RA and IR spectra of isolated thymine are from a

† Part of the special issue "Marilyn Jacox Festschrift".

* To whom correspondence should be addressed. E-mail: kperson@chem.ufl.edu; person@chem.ufl.edu.

‡ Present address: Surface Optics Corp., San Diego, California.

10.1021/jp994410p CCC: $19.00
Published on Web 03/30/2000

density functional theory (DFT) calculation using the B3LYP functional with a standard 6-31G(d,p) basis set. It is expected that the agreement between the calculated and experimental vibrational spectra from this calculation should be much better than were obtainable with earlier computational techniques (HF or even MP2) using the limited basis sets that are required in practical computations for such large molecules.[4] In addition to the routine calculation of optimized structures, vibrational frequencies, and IR and RA intensities, we have also calculated the potential energy distributions (PEDs) and IR and RA intensity distributions (IDs and RIDs) using programs written in our laboratory.

The main goals of the present work are: (1) To present and interpret the RA spectrum of matrix-isolated thymine. (2) To verify (or modify) existing assignments of the vibrational spectrum of isolated thymine, which were based only on the IR spectrum. (3) To obtain an experimentally verified, complete force field and set of intensity parameters for the isolated thymine molecule. (4) To compare the RA and IR spectra of isolated thymine with those of solid thymine, in order to establish a bridge between this work and previous studies made in the solid or in solution.

In a forthcoming publication we shall examine in detail the effects of hydrogen-bonding on the vibrational spectra and structure of thymine.

Methods

A. Experimental Procedures. A description of the experimental setup and details of the experimental procedure for the IR and RA studies has been given previously.[2] Here, we shall present a brief summary of the most necessary information.

Infrared Spectroscopic Studies. The experimental IR spectra of matrix-isolated thymine were obtained using a Nicolet Model 740 Fourier transform infrared (FTIR) spectrometer, at a spectral resolution of 1 cm^{-1}, with 200−500 scans. The high sensitivity and signal-to-noise ratio for this spectrometer allow the use of thin matrix samples, which we find to be much more uniform than those of thicker deposits. The spectrum recorded by the spectrometer was transferred to a PC for further data processing (e.g., to remove the interference fringes, to integrate the bands and decompose overlapping bands, and to plot the spectra) by the GRAMS[13] and SPECTRACALC[14] programs. The resulting spectra are shown in the figures.

A closed-cycle helium cryostat (Model DE-202 from APD Cryogenics, Inc.) cooled the sample holder to approximately 12 K. The cryostat chamber was evacuated to a pressure of about 10^{-7} Torr. Thymine (from Sigma Chemical Co.) was purified by vacuum sublimation during the process of forming the matrix sample. Polycrystalline thymine, in a small wire-wrapped glass tube placed inside the cryostat, was heated to sublimation at about 100 °C. This temperature is much lower than the decomposition point (335−337 °C).[15] A gaseous mixture of high-purity argon (introduced through a needle valve) and thymine vapor was deposited onto the cold CsI window. The concentration of thymine in the mixture was controlled by adjusting the temperature of the heater and the flow rate of the argon. The resulting matrix is dilute enough that no significant absorption due to self-associated molecules was observed, and it was thick enough to measure the absorption from very weak bands of monomeric thymine. The time needed to deposit matrices under these conditions was about 4−6 h.

Raman Spectroscopic Studies. The experimental study of the RA spectra of matrix-isolated molecules was performed using a Bruker Fourier transform spectrometer (IFS Model 66) equipped with the Raman station (FRA 106). The cryostat was similar to that used for the IR studies. Good quality RA spectra of matrix isolated thymine are much more difficult to obtain than are the corresponding IR spectra. To achieve better control of focusing the light on the matrix sample, a precisely controlled stage was built to move the entire cryostat in the incident beam. The argon + thymine vapor mixture was deposited on a solid aluminum block held in the coldfinger of the cryostat.

The excitation of the RA spectrum in the Bruker FT−Raman instrument was by the near-infrared line at 1.064 μm (or 9398.5 cm^{-1}) from a 3 W cw Nd:YAG laser (CVI Laser Co.). The light was focused onto the sample with the aid of a small mirror, and the backscattered light was collected. About 2000 scans at a resolution of 4 cm^{-1} were needed to ensure a high signal-to-noise ratio. The matrix was prepared in a manner similar to that used for the preparation of the matrix for the IR study. Deposition times from 6 to 10 h were needed to obtain matrix films thick enough to give a reasonable Raman scattering signal.

After recording the RA spectrum with the Bruker, it was transferred to the PC for data processing, including three corrections. First, the correction for the sensitivity of the spectrometer was introduced by multiplying the RA scattering signal by the instrumental response curve, according to the procedure described by Hendra, Jones, and Warnes.[16] The instrumental response curve is relatively flat for Raman shifts between 3400 cm^{-1} and 150 cm^{-1}, with a dramatic decrease of the response for shifts greater than 3400 cm^{-1} and smaller than 120 cm^{-1}, so reliable measurements of the spectra could be made only within this limit. Second, the scattering signal was corrected for the $\nu^4/\Delta\nu_{vib}$ factor.[16,17] The intensity of spontaneous Raman scattering increases with $\nu^4/\Delta\nu_{vib}$. Here, ν is the frequency of the scattered light ($\nu = \nu_{exc} - \Delta\nu_{vib}$, where ν_{exc} is the exciting light frequency = 9398.5 cm^{-1}); $\Delta\nu_{vib}$ is the observed Raman shift and is the frequency of the vibrational transition. Hence, the RA scattering signal was multiplied by a correction factor of $\Delta\nu_{vib}/\nu^4$, in addition to the correction described above for the sensitivity. The result of these two corrections gave a signal that could be integrated over each band to obtain the relative integrated band areas, which are directly proportional to the calculated "Raman scattering strengths" (the values of $[\partial\alpha/\partial Q]^2$) so that comparison between calculated and experimental relative values can be made. Third, the Raman scattering spectrum, corrected as described above, was adjusted further to obtain a horizontal baseline using the GRAMS or SPECTRACALC programs.[13,14] These programs were also used to decompose overlapping bands, integrate areas of the bands, and plot the final spectra.

The resulting experimental RA spectra are shown in the figures.

B. Theoretical Procedures. *Calculated Vibrational Spectra.* The optimized structure and vibrational spectra were calculated using GAUSSIAN 98W[18] on a PC (Dell Dimension XPS T450 with Pentium III processor). The DFT B3LYP/6-31G(d,p) calculations[19−21] were made first to optimize the structure and obtain the vibrational frequencies and IR intensities (integrated molar-absorption coefficients), and then they were continued to obtain the RA scattering strength of each band and, thus, the "calculated RA spectrum". The Cartesian force constants from the output of this calculation, together with the dipole moment and polarizability derivatives in Cartesian coordinates, were then transformed to their values expressed in internal and normal coordinates, as described below.

Transformation from Cartesian to Internal and Normal Coordinates. To describe the calculated normal vibrations in

terms of the internal (or symmetry) coordinates (i.e., the bond stretches (Δr) or changes in bond angles ($\Delta\alpha$)) familiar to the spectroscopist, it is necessary to transform the results given by GAUSSIAN 98W in Cartesian coordinates to the corresponding results expressed in terms of the internal coordinates. This transformation was done using programs written in our laboratory.[22] The transformations of force constants and dipole moment (or polarizability) derivatives are well-known and have been thoroughly discussed, for example, by Califano[23] and in papers by Mills.[24] The definitions of the internal coordinates abbreviated in the tables and the numbering of the atoms in thymine are the same as those given previously for thymine[3].

The most important reason to make this transformation to the internal coordinates is that the values of force constants and intensity parameters expressed in Cartesian coordinates depend on the orientation of the molecule with respect to the arbitrarily chosen Cartesian coordinate axes and, hence, are not transferable from one molecule to the other. This is not the case for the internal coordinates and the properties expressed using them. The bond force constants and dipole moment (or polarizability) derivatives expressed in the internal coordinates have a more obvious physical significance than is hidden in the atomic properties expressed in Cartesian coordinates. The usual description of normal modes of vibration is given in terms of the internal coordinates by the Potential Energy Distributions (PEDs),[23−25] which give the percentage contribution from each internal coordinate to the potential energy of the normal coordinate under consideration. The PEDs supplement the description of the normal mode as simply being a set of atomic displacements, as given in the GAUSSIAN programs, because the PEDs show explicitly how much of the total *energy* of the ν_s normal mode ($E = V_{max} = 1/2h\nu_s$) comes from each internal coordinate.

The PEDs for each normal mode of thymine are listed in the tables, which also summarize the frequencies, IR intensities, and RA scattering strengths calculated by the GAUSSIAN program. It should be noted that, with a few exceptions, small PED contributions have been omitted in these tables. For this reason, the PEDs shown in these tables for a given internal coordinate do not always sum over all normal coordinates to 100%, nor do all the PEDs for a given normal coordinate sum to 100%, because of the rounding error associated with this truncation of PEDs to show only values greater than 10%.

Using the coordinate transformations[22−24] and the values of the dipole derivatives expressed in the internal coordinates, it is possible to define the IR intensity distribution (ID) and, using the polarizability derivatives, the Raman intensity distribution (RID) for each normal mode. These quantities are analogous to the PED in that they give the contribution made by each internal coordinate to the total IR intensity, or total RA scattering strength, of each normal mode. The concept of IDs was discussed by Qian and Krimm.[26] Our programs[22] calculate the exact IDs and RIDs. The values are listed in the tables for each normal mode of thymine. The IDs (in km mol^{-1}) and RIDs (in Å^4 amu^{-1}) are defined to be the *absolute* contributions to the intensity, and are not normalized to 100%, as are the PEDs. Instead, the sum of exact IDs (or RIDs) for a given normal mode is the value of the calculated IR intensity (or RA scattering strength), if it were not for the rounding error due to the truncation in the tables, as discussed below.

Comparison of Calculated and Experimental Spectra. To compare the calculated and experimental spectra, it is useful to present the calculated data in a graphical form that is comparable to the experimental spectrum. We have used the GRAMS program to plot a simulated spectrum from the calculated data converted to an ASCA file by the ANIMOL program.[27] These spectra show each band with a Lorentzian shape, peaking at the calculated frequency, with its band height set equal to the value of the calculated IR intensity or RA scattering strength and with a constant width at half of the maximum intensity chosen to be 2 cm^{-1} for both IR and RA spectra.

The experimental values of the integrated IR intensities given in the tables are adjusted to be comparable with the calculated absolute integrated molar-absorption coefficients. The adjustment was made by multiplying the experimental integrated absorbance for each band in the experimental spectrum by a constant factor which brings the value of the integrated absorbance of one arbitrarily chosen experimental band (taken here to be the sum of the two C═O stretches responsible for the absorption from 1800 to 1700 cm^{-1}) into agreement with the calculated intensity sum of these bands. The physical meaning of this factor is that it is the reciprocal of the product of the concentration of the sample in the matrix by its path length (neither of which may be determined precisely but both are constant over the entire spectrum of a given sample). Hence, multiplication of the measured integrated absorbance for a band by this factor gives the experimental value of its absolute intensity (A, the absolute integrated molar absorption coefficient, in km mol^{-1}) by the Beer−Lambert law. These "experimental" values of the intensities of all bands are shown in the tables (later).

Similarly, the values of the "experimental" RA scattering strengths ($RASS_{exp}$) given in the tables were determined by multiplying each of the integrated RA scattering strengths obtained from the corrected Raman scattering signal, as described above, by the constant factor needed to bring the experimental integrated RA intensity of the RA band at 1683 cm^{-1} into agreement with the RA scattering strength ($RASS_c$) calculated for the "C5═C6 stretching" normal mode. This constant factor is related to the product of the concentration of the thymine and the volume of the matrix illuminated by the light.

The simulated calculated spectra are compared with the experimental spectra for thymine isolated in an Ar matrix in the figures shown later in this paper. The experimental RA spectra shown have been corrected for the instrument sensitivity and by the $\nu^4/\Delta\nu_{vib}$ factor to give the experimental RASS, as described above. Therefore, they are approximately comparable to the calculated RA scattering strengths ($RASS_c$) plotted as a function of the RA shift ($\Delta\nu_{vib}$) to give the "calculated RA spectra" shown in the figures. The corresponding numerical data are presented later in the tables.

Scaling the Force Constants from the Theoretical Calculation. Although the general agreement between the B3LYP/6-31G-(d,p) vibrational spectra and the experimental spectra is remarkable, a closer examination shows some discrepancy. Some of the discrepancy may be due to errors that might be correctable in a better calculation, but the most important reason is that the calculation is made under the harmonic approximation, and so, the calculated frequencies will be different from the corresponding experimental frequencies, which are not harmonic. One of the most convincing demonstrations of this, presented by Murphy et al.,[28] compared the MP2/6-31G* calculated spectra with the experimental spectra for trimethylamine and the deuterated derivatives. For thymine, we notice that the differences are largest for the NH- and CH-stretching region of the spectrum, in agreement with the knowledge that anharmonic

corrections for these normal modes are much larger than are those for other vibrations.[28−31]

To account for the anharmonicity of the experimental frequencies and normal modes, and also for some error in the calculation, we shall change the values of the calculated force constants to values estimated for the "effective anharmonic force constants". The concept of using "effective force constants" to predict experimental spectra, instead of "harmonic force constants", to predict the harmonic frequencies has been used implicitly (and explicitly) in almost every normal coordinate analysis that has ever been made. For thymine, the stretching of the terminal X−H and C═O bonds of the ring is expected to be quite anharmonic. The magnitudes of the anharmonic corrections ($2x_e\omega_e$) for some of these motions can be estimated from studies of other systems[28−32] and even more approximately from values listed by Herzberg[33] for diatomic molecules containing similar bonds.

The study by Murphy[28] provides reliable estimates for the anharmonicity corrections for all normal modes of the methyl group, including the HCH bending coordinates (scissors bends, umbrella bends, and rocking modes). The stretching modes have anharmonicity frequency corrections of about 120−140 cm^{-1} (∼4−5%), and the bending modes also have an appreciable anharmonicity correction (∼40 cm^{-1} or ∼3%, except for rocking modes for which it is ∼20 cm^{-1} or 2%). We expect anharmonicity corrections of about 5% of the frequency for NH and CO stretching motions,[32] somewhat less for in-plane bending of the NH bonds, and considerably less for most of the remaining modes of thymine.

To estimate the values of the "effective force constants" for the anharmonic displacements, we calculated the effective frequency, ν_{eff}, according to $\nu_{eff} = \nu_c - 2x_e\omega_e$. A diatomic molecule approximation is then used to estimate an effective force constant, k_{eff}, from the calculated value of the diagonal force constant, k_c, for the corresponding symmetry coordinate, by $k_{eff} = k_c \times (\nu_{eff}/\nu_c)^2$. This effective force constant then replaces the calculated diagonal (n,n) force constant for this n^{th} symmetry coordinate. The five "scaling factors" multiplying the calculated force constants that were adjusted for thymine were: (1) 0.902 for the N1H and N3H stretching force constants; (2) 0.911 for the C6H stretch and the 3 CH stretches of the methyl group; (3) 0.916 for the C2O and C4O stretches; (4) 0.946 for the C5C6 stretch; and (5) 0.950 for the N1H, N3H, and C6H bending force constants and the 3 methyl bends (umbrella, in-plane scissors, and out-of-plane scissors). All of the other diagonal and off-diagonal force constants from the calculation were used without scaling.

Results and Discussion

A comparison of the patterns of the experimental IR and RA survey spectra, with the corresponding calculated unscaled spectra, is shown for the full spectral range of this study in Figure 1. The general observations are as follows: (1) the IR and RA spectra from the B3LYP/6-31G(d,p) calculation have spectral patterns of frequencies and intensities that are very similar to those observed experimentally; and (2) the intensity distribution in the RA spectrum is very different from that in the IR spectrum, both in the calculated and experimental spectra. In the RA spectrum, most of the scattering strength appears in the region of the CH stretching modes (3200−2900 cm^{-1}), whereas the most intense absorption in the infrared spectrum is in the region of the carbonyl stretching modes (1800−1700 cm^{-1}). There are many examples in Figure 1 of bands that absorb weakly in the IR spectrum but scatter strongly in the RA spectrum, and vice versa.

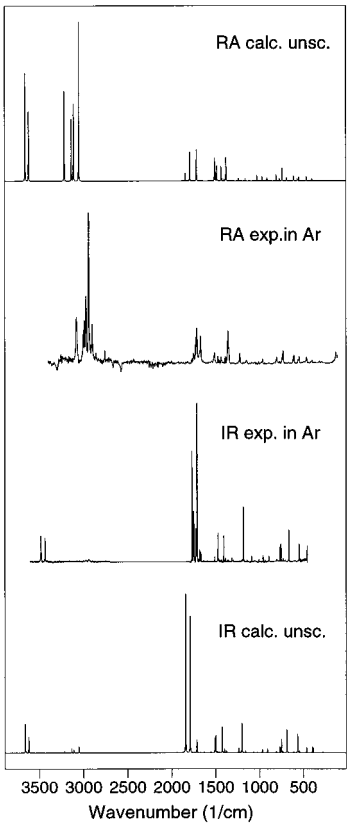

Figure 1. Comparison of the experimental Raman and infrared spectra, in the region from 3900 to 100 cm^{-1}, of thymine isolated in an Ar matrix at about 12 K, with the unscaled spectra from the B3LYP/6-31G(d,p) calculation. The vertical scale is linear in absorbance for experimental infrared spectra, in intensity for the calculated IR spectrum, and in RASS for the experimental and calculated RA spectra, as described in the text. The numerical values are given in the tables.

The following sections provide a description of the spectra in each spectral region and the analysis relating the experimental bands to the different vibrational modes of thymine expected in that region.

The NH, CH, CO, and CC stretching region (3700−1600 cm^{-1}). The experimental and calculated IR and RA frequencies and intensities for the six NH and CH normal modes of vibration, together with the two C═O stretching modes and the C5═C6 stretching mode in this region are listed in Table 1 and the spectra are plotted in Figures 2 and 3. The left side of this table lists under "unscaled calculation" the results from the B3LYP/6-31G(d,p) calculation at the harmonic approximation for the frequency, ν_c, and the IR and RA activities, A_c and $RASS_c$, together with the calculated PEDs, IDs, and RIDs, obtained as described above. On the right side of the table the corresponding values calculated from the set of "scaled force constants" described in the previous section are given in italicized type. The experimental frequencies, ν_{exp}; total relative integrated infrared intensities, A_{exp}; and total relative integrated Raman scattering strengths, $RASS_{exp}$, for each band, measured as described above, are shown in boldfaced type on the right side of Table 1, under the calculated scaled values.

NH and CH Stretching Vibrations (3700−2800 cm^{-1}). The assignment of the experimental bands to the calculated normal modes is almost obvious. The highest frequency experimental bands observed in the IR spectrum (3479 and 3432 cm^{-1}) are assigned to the N1H- and N3H-stretches, respectively. (Note that in the RA studies, these frequencies fall outside the region

TABLE 1: Comparison of the Calculated and Scaled Frequencies, ν_c and ν_{scaled} in cm^{-1}, Calculated IR Intensities, A_c in km Mol^{-1}, and Raman Scattering Strengths, $RASS_c$ in Å^4 Amu^{-1}, with the Corresponding Experimental Values (in bold) in the 3500−1650 cm^{-1} Region for Thymine in an Ar Matrix[h]

Unscaled calculation					Scaled calculation			
Q_s	ν_c	A_c	$RASS_c$	Assign (PED) [ID]{RID}[f]	ν_{scaled}[a] ν_{exp}[b]	A_c $\mathbf{A_{exp}}$	$RASS_c$ $\mathbf{RASS_{exp}}$	Assign (PED) [ID]{RID}[f]
1	3659	97	105	N1H s (100−) [89] {109}	*3475*	*97*	*106*	*N1H s (100−) [89] {109}*
					3479(IR)	**130**	*c*	
2	3619	63	81	N3H s (100−) [59] {84}	*3437*	*63*	*81*	*N3H s (100−) [59] { 84}*
					3432(IR)	**110**	*c*	
3	3214	6	91	C6H s (100+) [5] {99}	*3067*	*7*	*91*	*C6H s (99+) [5] {99}*
					3078(RA)	**74**		
4	3133	15	66	aMeCH s (100+) [14] {70}	*2989*	*15*	*65*	*aMeCH s (100+) [14] {70}*
					2997(RA)	**42**[d]		
					2992(IR)	**7**		
5	3109	12	87	oMeCH s (100+) [12] {87}	*2967*	*12*	*86*	*oMeCH s (100+) [12] { 87}*
					2969	**13**	**55**	
6	3050	22	167	sMeCH s (100+) [23] {165}	*2910*	*22*	*167*	*sMeCH s (100+) [22] {165}*
					2939	**20**	**162**[d]	
7	1842	643	9	C2O s (73+) [455] {22}	*1774*	*686*	*7*	*C2O s (69+) [462] {19}*
				C2N3 s (5−) [76] {−4}	**1767**	**617**[d]	**12**[d]	*C2N3 s (6−) [83] {−4}*
				N1C2 s (4−) [81] {−3}				N1C2 s (5−) *[84] {−3}*
8	1791	488	30	C4O s (78+) [338] {38}	*1722*	*498*	*35*	*C4O s (70+) [329] {39}*
				N3C4 s (2−) [52] {−5}	**1711**	**492**[d]	**46**[d]	*N3C4 s (2−) [51] {−6}*
9	1715	44	32	C5C6 s (62+) [41] {42}	*1673*	*14*	*27*	*C5C6 s (57+) [23] {34}*
				C6H be(12−) [−6] {−1}	**1668**	**66**[d]	**32**[d,e]	*C6H be (11−) [−3] {0}*
				N1C6 s (6−) [23] {−2}				*C4O s (8−) [−16] {−6}*
				C4O s (3−) [−17] {−4}				*N1C6 s (7−) [11] {−2}*

[a] For discussion of the scaling factors for the force constants, see text. [b] (IR) or (RA) next to the frequency indicates that the band is observed only in the IR or RA spectrum. [c] Not possible to measure; the instrumental sensitivity is too small in this region. [d] The total relative intensity for all of the subbands observed for this mode (see Figure 2 and text). [e] Reference for the relative RASS values. See text. [f] All of the values for PEDs, IDs, and RIDs truncated at the 10% level, except for selected normal modes. [g] For these selected modes, all PEDs, IDs, and RIDs greater than 1 are shown. The total sum of PEDs is shown equal to 100% (within rounding error); the sum of IDs is equal to A_c and the sum of RIDs is equal to $RASS_c$, also within the rounding errors. [h] The experimental values for the IR intensity, $\mathbf{A_{exp}}$, and Raman scattering strengths, $\mathbf{RASS_{exp}}$ are *relative* values, as discussed in the text. The assignment of the experimental spectrum is made using this comparison and lists here the calculated contributions to the potential energy, PED in percent, to the infrared intensity, ID in km mol^{-1}, and to the Raman scattering strength, RID in Å^4 amu^{-1}, from each internal coordinate for each normal mode.

of sensitivity of our instrument.) The experimental ratio of *integrated* infrared intensities (A_1(N1H)/A_2(N3H) = 1.48) for these bands is very close to the calculated ratio (1.53), despite the qualitative appearance of the intensity *maxima* in Figure 2. The difference between the experimental and calculated NH-stretching frequencies is about 180 cm^{-1}, only 20−40 cm^{-1} higher than the anharmonicity correction of the NH-stretch measured for pyrrole (about 140 cm^{-1}),[32] for HN_3 (about 156−161 cm^{-1}),[30] and for NH_3 (about 148 cm^{-1}).[29]

The CH-stretching modes show very intense RA scattering, but their IR absorption is barely observable. Consequently, the assignment given in Table 1 for these modes is made mostly on the basis of the comparison of the relative experimental RA scattering strengths with the calculation. The experimental band at 3078 cm^{-1} was assigned to the C6H-stretching mode. The doublet at 2987 and 2997 cm^{-1} is assigned to the asymmetric in-plane CH-stretching vibration of the CH_3 group. This doublet results from Fermi resonance between the unperturbed fundamental and a combination band (e.g., 1220 cm^{-1} + 1767 cm^{-1} = 2987 cm^{-1}). The experimental band at 2969 cm^{-1} is assigned to the out-of-plane asymmetric CH stretching mode of the CH_3 group. Finally, the strongest RA scattering in the experimental spectrum, at 2939 cm^{-1}, together with the weaker band at 2899 cm^{-1} (Fermi resonance with 2 × 1472 cm^{-1}) is assigned to the symmetric CH-stretching mode of the methyl group. For all CH stretching vibrations discussed above, the difference between the calculated harmonic and the experimental frequencies is on the order of the expected anharmonic correction.[28,31] The spectra calculated after scaling the stretching force constants by just the two scaling factors applicable to this region (0.902 for k_{NH} and 0.911 for k_{CH}, as described above) given on the right side of Table 1 and shown in Figure 2 are very close to the experimental spectra.

CO and CC Stretches (1900−1600 cm^{-1}). The values of the experimental and calculated frequencies and intensities for the CO and CC stretching modes are also listed in Table 1, and the spectra are shown in Figure 3. The assignment of the experimental bands in this region is less straightforward because there are many more bands in the experimental spectrum than expected from the three normal modes predicted by the calculation. Such highly structured IR spectra are commonly observed for matrix-isolated pyrimidines in this region, and have been reported previously in the IR spectrum of matrix-isolated thymine and uracils.[2−5,10−12,34,35] The structure is generally believed to result from the Fermi resonance between a fundamental carbonyl stretching vibration and combination bands involving the lower frequency modes. We agree with this interpretation and propose some possible combination bands in the caption of Figure 3 that may appear in Fermi resonance with the C═O stretching modes.

The intense band at 1767 cm^{-1} in the experimental IR spectrum, together with the two weaker bands at 1751 and 1745 cm^{-1}, are all believed to derive their intensity from the C2═O stretching mode. The corresponding bands from this normal mode in the experimental RA spectrum appear at 1767 and 1748 cm^{-1} (1751 and 1745 cm^{-1} bands overlapped at the lower resolution of the RA spectrum). The bands at 1724−1711 cm^{-1} in both the experimental IR and the experimental RA spectra are assigned to the C4═O stretching vibration and its Fermi resonance components.

Finally, the intense RA band observed at 1668 cm^{-1} (with a shoulder at about 1683 cm^{-1}) and the two very weak IR bands

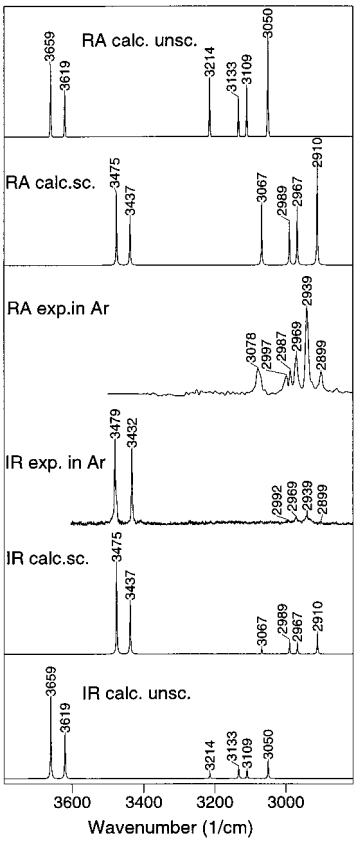

Figure 2. Comparison of the experimental Raman and infrared spectra in the NH and CH stretching region (3700−2700 cm^{-1}), of thymine isolated in an Ar matrix at about 12 K, with the unscaled, and with the scaled (described in the text), spectra from the B3LYP/6-31G(d,p) calculation. The vertical scale is described in the caption for Figure 1.

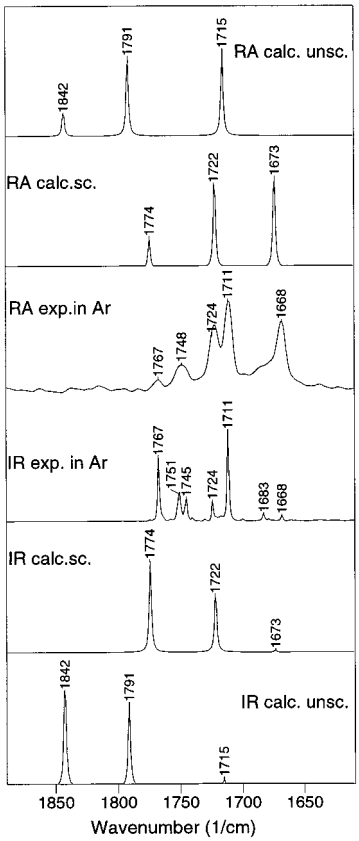

Figure 3. The same comparison of experimental and calculated spectra described in the caption for Figure 2, except this figure shows the double-bond stretching spectral region (1800−1600 cm^{-1}). Combinations of lower frequency modes (in cm^{-1}) that might be involved in Fermi resonance with the fundamentals in this region include: (959 cm^{-1} + 799 cm^{-1} = 1758 cm^{-1}); (1472 cm^{-1} + 282 cm^{-1} = 1754 cm^{-1}); (1183 cm^{-1} + 540 cm^{-1} = 1723 cm^{-1}); (1405 cm^{-1} + 282 cm^{-1} = 1687 cm^{-1}); (1220 cm^{-1} + 455 cm^{-1} = 1675 cm^{-1}).

at 1668 and 1683 cm^{-1} (Fermi-resonance doublet) are assigned to the C5═C6 stretching mode. The calculated frequencies of the C2═O and C4═O stretching modes are both higher than the experimental frequencies, by about 80 cm^{-1}, and this difference for the C5═C6 stretch is about 40 cm^{-1}. All of these differences are on the order of the expected anharmonicity corrections.[32]

We note that scaling the force constants as described above has a very small effect on the PEDs, IDs, and RIDs of the normal modes and calculated spectrum on the right side of Table 1, compared to the unscaled spectrum on the left side. The different scale factors used for the C5═C6 and C═O force constants have some effect on the mixing of these symmetry coordinates in the normal modes and, thus, some effect on their relative intensities. Some indication of the magnitude of this effect for these quantities is shown in Table 1.

Even though the predominant contribution (about 70−80%) to the potential energy of the normal modes comes from the C2═O (or C4═O or C5═C6) stretching coordinates in the respective normal modes (see the PEDs in Table 1), the calculated displacements of the atoms in these normal modes show sizable movements of the hydrogen atoms attached at the N1 and N3 positions as bending of the N1−H and N3−H bonds. A similar observation was made by Aida et al.[6] These displacements appear to be "reflex motions" of the light hydrogen atom, as a result of the motion of the heavy carbon and nitrogen atoms, as shown in Figure 4. Their involvement in "C2O and C4O stretching normal modes" probably does account for the strikingly different spectral pattern in this carbonyl region for the N1,N3-dideuterated thymine (see ref 10).

CH-bending, NH-bending, and Ring modes (1600−1300 cm^{-1}). The experimental IR and RA spectra are compared with the calculated spectra in Table 2 and plotted in Figure 5. The B3LYP/6-31G(d,p)-calculated unscaled IR and RA spectra are shown at the bottom and top of Figure 5, respectively. Although the unscaled calculated frequencies of bands in this region are not very different from those in the experimental spectra, the spectral patterns are strikingly different.

Examination of Table 2 shows that seven normal modes are expected in this region, with principal contributions to PEDs from the HCH umbrella and in-plane and out-of-plane scissors bending coordinates of the methyl group and the N1H and N3H in-plane bending, ring stretching, and C6H in-plane bending coordinates of thymine. The seven internal coordinates mix to give rather complicated normal modes, as can be seen from the PEDs for the "unscaled calculation" on the left side of Table 2.

The intensity pattern from this unscaled B3LYP/6-31G(d,p) calculation has three strong IR bands at 1510, 1499, and 1426 cm^{-1}, whereas only two are observed experimentally at 1472 and 1405 cm^{-1}. It seems that the unscaled force constants calculated for the methyl group bending coordinates, and also for the NH and C6H in-plane bending coordinates, are too high relative to the force constants calculated for the ring stretching internal coordinates. As discussed previously, it appears that it is necessary to scale the force constants for the CH and NH in-plane bends by 0.95 to account, primarily, for the expected anharmonicity corrections in these coordinates. The resulting

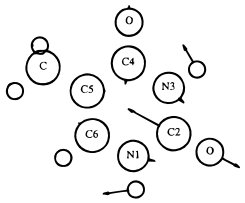

ν(calc uns)=1842 cm^{-1}; ν(exp)=1767 cm^{-1}

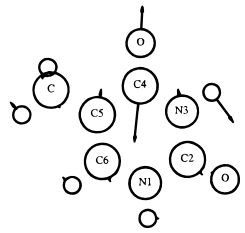

ν(calc uns)=1791 cm^{-1}; ν(exp)=1711 cm^{-1}

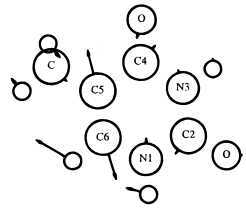

ν(calc uns)=1715 cm^{-1}; ν(exp)=1668 cm^{-1}

Figure 4. Atomic displacements calculated (B3LYP/6-31G(d,p)) for the "C2═O, C4═O, and C5═C6-stretching" normal modes. The atomic displacements were plotted using the ANIMOL program,[27] as described in the text.

frequency and intensity patterns are shown as the "scaled IR" and "scaled RA" spectra in Figure 5 and on the right side of Table 2.

As can be seen in Table 2 and Figure 5, the calculated IR and RA spectra using the scaled force constants are noticeably in better agreement with the experimental spectra. The degree of mixing of the internal coordinates in the normal modes depends very much on the relative values of the force constants, as can be seen from the PEDs from the "scaled force constant" calculation shown on the right side of Table 2. The assignment of the experimental spectrum in Table 2 has been based on the "scaled force constant" calculation of the IR and RA spectra in this region, which seems to us to be more consistent with the characteristic frequencies of methyl group vibrations (compare, for example, with Murphy et al.[28]). The main discrepancy between the experimental and scaled (or unscaled) calculated RA spectra appears to be the overestimation in the calculation of the RA scattering strength for most of the bending modes of the methyl group.

The assignment of the band in the IR and RA spectra at 1510 cm^{-1} needs some discussion. This band is quite weak in the IR spectrum and has been assigned in previous studies[10] to an overtone. We interpret this band as an overtone, $2\nu_{26}$ (2×754 cm^{-1} = 1508 cm^{-1}) or combination, $\nu_{17} + \nu_{36}$ (1220 cm^{-1} + 282 cm^{-1} = 1502 cm^{-1}). However, its relatively high RASS is surprising and suggests its possible coupling with the band observed at 1472 cm^{-1}.

It is also of some interest to investigate the contributions to the IR and RA intensities of each of these seven normal modes from each internal coordinate by examining the IDs and RIDs in Table 2 to discover how they change when the force constants are scaled. Aida et al.[6] pointed out the remarkably strong Raman scattering observed in solid thymine at 1368 cm^{-1}, attributed to the C6H bending mode and offered an explanation based on their calculations.[7] We note that a very strong band is also observed near this frequency (at 1357 cm^{-1}) in the RA spectrum of matrix-isolated thymine. The assignment of this band from the "unscaled calculation", given in terms of the PED contributions, is "38% C6H be, 15% N3H be, and 11% C5C6 s", or the slightly different description from the "scaled calculation".

We may examine the relative importance of the contributions from each symmetry coordinate to the IR or RA intensities using the IDs (for IR intensity) and RIDs (for RA intensity). The results are presented in Table 2 for the normal mode assigned to this strong RA band ν_{16}, for both the "unscaled" and "scaled" calculations. Ignoring for the moment the small differences between the scaled and unscaled calculations, we shall use the results from the unscaled calculation to illustrate the use of the RIDs to explain the source of the large RASS for this band.

These RIDs show that the total calculated RASS, of 25 Å^4 amu^{-1}, results from several contributions. The RASS is so high because the ring-stretching coordinates combine to give a motion that expands the ring, which contributes ~50% of the total intensity and is in-phase with that from the C6H bending (about 25%) and also with a number of other smaller contributions, including C4O stretching. The coordinates that contribute relatively strongly to the RASS do not contribute very much to the potential energy of the normal mode. For example, the C5C6 stretching motion contributes 40% of the RASS but only 11% of the potential energy. In contrast to the RA activity, all of the contributions to the IR intensity (the IDs) are very small for this mode.

Ring Stretching and Bending Modes, In-Plane and Out-of-Plane Bending Modes (1300−100 cm^{-1}). The IR and RA spectra below 1300 cm^{-1} are shown in Table 3 and plotted in Figures 6 and 7. We see in Table 3 that 23 fundamental modes are expected in this region. They arise from several different types of internal coordinates (or "local modes"). Comparison of the IR and RA spectra in this region provides very helpful confirmation of the identification of the fundamental modes in the experimental spectrum. For example, the absorption in the IR spectrum by the bands at 1220 and at 601 cm^{-1} is almost undetectable, but both have relatively strong RA scattering strengths.

The close agreement of the spectra from the "unscaled calculation" (B3LYP/9-31G(d,p) with no scaling) with the experimental IR and RA spectra in this region seen in Figure 6 makes the assignment relatively routine. This assignment of the experimental spectra is given in Table 3.

Some small differences in frequencies in this region from "unscaled" calculations and experiment might result from mixing of NH and CH bending and CO stretching internal coordinates (with larger anharmonicity, as described above) in several of the normal modes in this low-frequency region. These differences (approximately 1−20 cm^{-1}) do not lead to any uncertainty in the assignment. As has been observed for the other regions of the spectrum, several absorption bands are observed in the IR spectrum (for example, at 1315, 1297, 1197, and 1190 cm^{-1}) that are not matched by corresponding RA shifts. These bands can be assigned to combination and overtone bands, e.g., $2\nu_{28}$ (2×662 cm^{-1} = 1324 cm^{-1}), $\nu_{26} + \nu_{30}$ (754 cm^{-1} + 545 cm^{-1} = 1299 cm^{-1}), $\nu_{28} + \nu_{30}$ (662 cm^{-1} + 545 cm^{-1} = 1209 cm^{-1}), and $2\nu_{29}$ (2×601 cm^{-1} = 1202 cm^{-1}), respectively.

Examination of the Intensities of Selected Bands. The examination of the reasons for the high RASS of the 1357 cm^{-1} band given in the previous section has suggested to us the value

TABLE 2: Comparison of Calculated and Experimental Spectra of Thymine in an Ar Matrix in the 1600−1250 cm^{-1} Region[h]

Unscaled calculation					Scaled calculation			
Q_s	ν_c	A_c	$RASS_c$	Assign (PED) [ID] {RID}[f]	ν_{scaled}[a] ν_{exp}[b]	A_c $\mathbf{A_{exp}}$	$RASS_c$ $\mathbf{RASS_{exp}}$	Assign (PED) [ID]{RID}
10	1510	50	23	Me sci (59−) [10] {12}	*1469*	*12*	*12*	*Me sci (72−) [−5] {11}*
				N1C6 s (9−) [21] {−1}	**1455**	**7**[d]	**4**	
				C2O s (2+) [−14] {3}				
				N1C2 s (1+) [10] {1}				
				C4O be (1+) [10] {1}				
11	1499	64	10	N1H be (28−) [18] {1}	*1487*	*114*	*20*	*N1C6 s (18−) [46] {−2}*
				Me sci (27−) [−5] {3}				*N1H be (17+) [21] {3}*
				N1C6 s (12+) [32] {0}	**1472**	**115**[d]	**16**[d]	*Me sci (13−) [7] {4}*
				N1C2 s (7−) [24] {0}				*C4C5 s (10+) [5] {2}*
				C2O s (7−) [−29] {3}				*Ri def 3 (8−) [−17] {6}*
				Ri def 3 (5+) [−10] {3}				*N1C2 s (7+) [33] {2}*
				N3C4 s (3+) [12] {0}				*C2O s (7+) [−38] {7}*
				C4O be (2−) [15] {1}				*N3C4 s (5−) [18] {−5}*
								C4O be (3+) [30] {3}
12	1483	6	18	o Me sci (92+) [7] {14}	*1449*	*6*	*18*	*o Me sci (91+) [7] {14}*
					1431	**11**[d]	**7**	
13	1435	2	16	Me umb(93+) [−1] {18}	*1397*	*4*	*18*	*Me umb (94+) [1] {19}*
					1388	**7**	**5**	
14	1426	90	3	N1H be(18+) [−18] {1}	*1412*	*72*	*2*	*N1H be (28+) [−21] {1}*
				C2N3 s (18+) [−3] {3}				*C2N3 s (18+) [−1] {1}*
				C4C5 s (13−) [14] {0}	**1405**	**71**[d]	**1**	*C2O be (12+) [39] {0}*
				C2O be (9+) [38] {−1}				*C4C5 s (7−) [10] {0}*
				C4O be (8−) [38] {−2}				*C4O be (7−) [30] {−1}*
				N1C2 s (6−) [24] {0}				*N1C2 s (6−) [20] {1}*
				C2O s (4+) [14] {2}				*C2O s (6+) [14] {1}*
				Ri def 3 (3+) [−11] {−2}				
				C4O s (3−) [−10] {0}				
15	1400	13	2	N3H be (50+) [2] {0}	*1370*	*4*	*5*	*N3H be (39+) [0] {0}*
				C6H be (11−) [0] {0}	**1367**	**2**	**3**	*C6H be (21−) [0] {1}*
				C2O be (7+) [10] {1}				
16[g]	1379	8	25	C6H be (38−) [0] {7}	*1352*	*4*	*24*	*C6H be (26−) [0] {6}*
				N3H be (15−) [0] {1}	**1357**	**6**[d]	**31**[d]	*N3H be (24−) [0] {2}*
				C5C6 s (11−) [−4] {11}				*C5C6 s (9−) [−2] {10}*
				C2N3 s (8+) [0] {−4}				*C2N3 s (8+) [0] {−3}*
				N1C2 s (6−) [6] {4}				*N1H be (7−) [2] {0}*
				N1H be (4−) [3] {0}				*N3C4 s (6−) [−1] {4}*
				Me sci (3+) [1] {2}				*N1C2 s (4−) [4] {3}*
				C4C5 s (3+) [−3] {0}				*C4C5 s (4+) [−2] {0}*
				C5Me be (3-) [−2] {−1}				*Me sci (3+) [1] {2}*
				Me ro (3−) [0] {−1}				*Me ro(2−) [0] {−1}*
				N3C4 s (2−) [−1] {3}				*C5Me be (2−) [−1] {−1}*
				C4O be (1−) [2] {0}				*C2O s (2+) [2] {−1}*
				C2O s (1+) [2] {0}				*C4O s (1−) [−1] {3}*
				C5Me s (1+) [0] {0}				*C4O be (0−) [1] {0}*
				Ri def 2 (1+) [0] {1}				*C2O be (0−) [1] {1}*
				C4O s (1−) [−1] {2}				***Total (98) [4]*** {***25***}
				C2O be (0−) [4] {1}				
				Total (101) [7] {**26**}				

[a] For discussion of the scaling factors for the force constants, see text. [b] (IR) or (RA) next to the frequency indicates that the band is observed only in the IR or RA spectrum. [c]Not possible to measure; the instrumental sensitivity is too small in this region. [d] The total relative intensity for all of the subbands observed for this mode (see Figure 2 and text). [e] Reference for the relative RASS values. See text. [f] All of the values for PEDs, IDs, and RIDs truncated at the 10% level, except for selected normal modes. [g] For these selected modes, all PEDs, IDs, and RIDs greater than 1 are shown. The total sum of PEDs is shown equal to 100% (within rounding error); the sum of IDs is equal to A_c and the sum of RIDs is equal to $RASS_c$, also within the rounding errors. [h] The experimental values for the IR intensity, $\mathbf{A_{exp}}$, and Raman scattering strengths, $\mathbf{RASS_{exp}}$ are *relative* values, as discussed in the text. The assignment of the experimental spectrum is made using this comparison and lists here the calculated contributions to the potential energy, PED in percent, to the infrared intensity, ID in km mol^{-1}, and to the Raman scattering strength, RID in Å^4 amu^{-1}, from each internal coordinate for each normal mode.

of similar discussion of some of the stronger bands in the experimental IR and RA spectra in this region. In particular, consider the bands observed at 1183, 763, 754, 662, and 545 cm^{-1} in the IR spectrum and the strong RA band observed at 727 cm^{-1}. Except for the carbonyl stretching modes, the band (ν_{18}) at 1183 cm^{-1} is the strongest band in the IR spectrum of thymine isolated in the Ar matrix. The band at 727 cm^{-1} is very weak in the IR spectrum but is the strongest band observed in this region of the experimental RA spectrum. Table 3 gives the expanded (1% level) PED, ID, and RID descriptions of these six normal modes.

The reason for the very high IR intensity of ν_{18}, observed at 1183 cm^{-1}, is revealed in the IDs of the expanded description for this mode given in the right side of Table 3. The intensity (112 km mol^{-1}) comes primarily from in-phase ring stretches with contributions from C6H and N3H bends canceling each other but with a small contribution from the C2O bend. The intensity is so high because these motions occur in-phase, so that the largest contributions to the IR intensity add together.

Now let us examine the relatively strong pair of bands observed in the IR spectrum at 763 and 754 cm^{-1}. There has been some controversy over their assignment, but it is clear

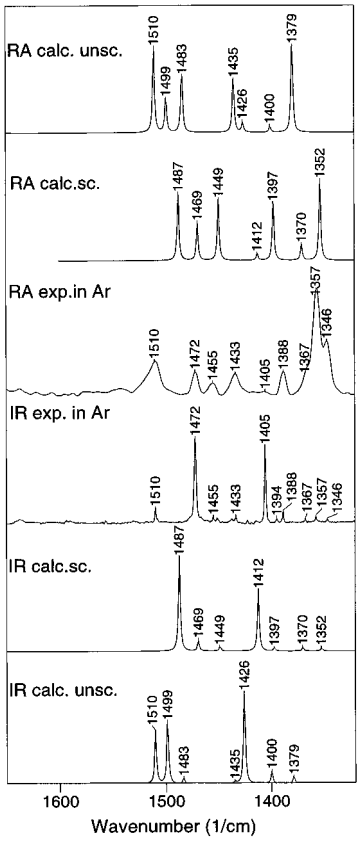

Figure 5. The comparison is similar to that described in the caption for Figure 2, but is in the spectral region from 1600 to 1320 cm^{-1}.

from the PEDs in Table 3 that the band at 763 cm^{-1} is mostly the out-of-plane C4O wagging mode, and that at 754 cm^{-1} has its main contribution from the out-of-plane wag of C2O.

The IR intensity (20 km mol^{-1}) calculated for the 763 cm^{-1} band is explained by major contributions from the out-of-plane C4O wag and the out-of-plane N3H wag, with a smaller contribution from the out-of-plane ring deformation 3, partly canceled by a large negative contribution from the out-of-plane ring deformation 1. Similarly, the IR intensity (52 km mol^{-1}) of the 754 cm^{-1} band is explained by a major contribution from the out-of-plane C2O wag, adding in phase to the large NH wagging contributions, canceled by the large negative (out-of-phase) contributions by the out-of-plane ring deformations 1 and 3.

Each infrared ID in these modes is very large, and the relatively small total intensity is the result of their cancellation in the normal mode because of the phase differences. The infrared ID analysis shows very clearly that the prediction of accurate force constants is essential to show exactly the cancellation of the opposing contributions to the intensity.

For the strong RA mode at 727 cm^{-1}, the largest value in the PED description in Table 3 is for the C4C5 stretch, with a considerably smaller PEDs from the methyl group stretching against the C5 atom and from in-plane distortion of the ring (Ri def 3). Other ring-stretching coordinates make minor contributions to the potential energy. In contrast, we see that the explanation for the calculated value of the RASS is a dominant contribution from the in-phase ring stretching coordinates, which collectively describe a "ring-breathing" motion, with additional minor contributions from C5Me and C4O stretches that are partly canceled by a small contribution from Ri def 3. The high RASS is found because most contributions add in-phase. This mode is another example showing that Raman RIDs from internal coordinates with small PEDs are often important in determining the RA scattering strength.

These examples illustrate the use of calculated PEDs, IDs, and RIDs in the interpretation of the vibrational spectra of matrix-isolated thymine. The values given in the Tables may be used for detailed interpretation of other normal modes but need not be discussed further here.

The Low-Frequency Region. Below 450 cm^{-1} (Figure 7), the sensitivity of our IR spectrometer is too small for measurements, and the experimental RA spectra alone provide information about the lower frequency vibrational spectrum. Even there, the sensitivity of our Raman spectrometer is too small to measure significant scattering for Raman shifts below 125 cm^{-1}.

The assignment of the experimental bands at 307 and 282 cm^{-1} to the normal modes calculated at 300 and 278 cm^{-1} is obvious. However, only one band is observed in the experimental RA spectrum at 391 cm^{-1} (although with a weaker shoulder at 407 cm^{-1}), whereas the unscaled calculation predicts two bands, a stronger band at 397 cm^{-1}, related mainly to the out-of-plane ring deformation 1 and 3 and a weaker band calculated at 387 cm^{-1}, corresponding to the in-plane C2O and C4O bending mode. It is possible that force constants for in-plane and out-of-plane coordinates should be scaled slightly differently, which might reverse the order of the calculated frequencies.

The RA scattering by the two bands reported experimentally at 155 and 139 cm^{-1} is very weak, and hardly distinguishable from the noise level; hence, their assignment as fundamentals in Table 3 is very uncertain. We assigned these two bands to the modes calculated at similar frequencies associated with the out-of-plane ring deformations 1, 2, and 3 and to the methyl torsion, respectively. We believe that the assignment by Aamouche et al.[9] of the low-frequency spectrum of solid thymine may provide the best guide to the assignment also for the isolated thymine of this study (see the next section).

Comparison of the IR and RA Spectra of Thymine Isolated in an Ar Matrix with those of the Polycrystalline Solid. Although the main subject of this study has been to measure and interpret the experimental vibrational spectra of isolated thymine, we believe that it is useful to show how these spectra compare with the spectra of solid thymine studied with the same instruments. This is particularly important for the RA spectra because the previous studies of these spectra have been made experimentally for solids or solutions, but the interpretation has been based on quantum-mechanical calculations made for the isolated molecule. Figure 8 presents such a comparison of IR and RA spectra for matrix-isolated thymine with those for a polycrystalline solid sample.

Examination of Figure 8 reveals that the pattern in the RA spectrum of polycrystalline thymine is, in general, strongly similar to that for the thymine isolated in the Ar matrix, except for the region of the double-bond stretches (1800−1600 cm^{-1}). This observation is in sharp contrast with the comparison of IR spectra for the two systems. The explanation for this difference between the effect of the hydrogen-bonding interaction in the solid on RA and IR spectra is probably related to the fact that the contributions to RA scattering strength from the internal coordinates, which are strongly affected by hydrogen bonding (e.g., NH stretching and bending coordinates), are very small, and possibly decreased because of interaction. The internal coordinates that do have large contributions to the RA scattering strength (e.g., CH stretches and bends, and ring modes) are not strongly affected by hydrogen bonding.

TABLE 3: Comparison of Calculated and Experimental Spectra in the 1250−100 cm^{-1} Region of Thymine in an Ar Matrix[h]

Unscaled calculation					Unscaled calculation				
Q_s	ν_c ν_{exp}[b]	A_c $\mathbf{A_{exp}}$	$RASS_c$ $\mathbf{RASS_{exp}}$	Assign (PED) [ID]{RID}[f]{RID}[f]	Q_s	ν_c ν_{exp}[b]	A_c $\mathbf{A_{exp}}$	$RASS_c$ $\mathbf{RASS_{exp}}$	Assign (PED) [ID]{RID}[f]{RID}[f]
17	1236	16	2	C5Me s (31+) [0] {1}	27[g]				N1C2 s (6−) [2] {2}
	1220	**4**	**6**	N1C6 s (19−) [22] {−1}					C5C6 s (6−) [−1] {3}
				Ri def 1 (12+) [1] {1}					N1C6 s (4−) [−1] {0}
				N1C2 s (9+) [10] {2}					C2N3 s (3−) [0] {1}
				C2N3 s (9−) [−11] {−1}					C2O be (2−) [−2] {0}
18[g]	1201	112	0	C6H be (20−) [8] {−1}					C4O s (2−) [−1] {1}
	1183	**124**	**1**	N1H be (18+) [1] {0}					N3H be (1+) [0] {0}
				N1C6 s (18+) [39] {0}					C4O be (1−) [2] {0}
				C2N3 s (16−) [35] {0}					***Total (100) [3]*** {***13***}
				N3C4 s (12+) [35] {0}	28[g]	686	83	3	o N3H wag (86+) [85] {3}
				N3H be (6−) [−8] {0}		**662**	**70**	**0**	o Ri def 1 (19+) [23] {1}
				C5Me s (3−) [1] {0}					o N1H wag (1−) [3] {0}
				C4C5 s (2−) [−8] {0}					o C2O wag (0−) [−14] {0}
				C2O be (2−) [11] {0}					o C6H wag (−1+) [2] {0}
				Me ro (1+) [1] {0}					o C4O wag (−1+) [-4] {0}
				Total (98) [115] {***−1***}					o Ri def 2 (−1+) [1] {0}
19	1159	6	2	N3C4 s (31−) [4] {2}					o Ri def 3 (−4−) [−11] {0}
	1139	**7**	**3**	N1C6 s (13+) [−4] {0}					***Total (99) [85]*** {***4***}
				Me ro (10+) [0] {1}	29	606	1	5	C2O be (27−) [−2] {2}
20	1071	2	0	o Me ro (81−) [1] {1}		**601**	**1**	**7**	C4O be (23−) [3] {0}
	1046	**1**	**1**	o C5Me wag (11−) [0] {0}					C5Me be (14−) [−1] {1}
21	1026	2	5	Me ro (52+) [1] {3}					Ri def 2 (12−) [0] {1}
	1004	**4**	**3**	Ri def 1 (16−) [0] {1}	30[g]	563	63	2	o N1H wag (91−) [75] {2}
22	966	10	4	N1C2 s (27−) [11] {2}		**545(IR)**	**52**		o N3H wag (4+) [−17] {0}
	959	**10**	**3**	Me ro (13+) [1] {1}		**551(RA)**	**3**[d]		o C4O wag (3+) [7] {0}
				C2N3 s (12−) [4] {1}					o Ri def 2 (2−) [0] {0}
23	910	14	4	o C6H wag (100+) [16] {4}					***Total (100) [65]*** {***2***}
	889	**20**	**1**	o Ri def 3 (−5−) [−10] {0}	31	545	7	4	Ri def 3 (30+) [2] {2}
24	805	4	6	Ri def 1 (45+) [0] {2}		**540**	**8**	**3**	Ri def 2 (24+) [2] {0}
	799	**10**	**5**	C5Me s (19−) [0] {−1}					C4O be (12−) [−3] {1}
				N1C2 s (12+) [−4] {2}	32	460	18	4	Ri def 2(43+) [5] {2}
25[g]	767	20	2	o C4O wag (80−) [26]{−1}		**455**	**10**	**4**	Ri def 3 (30−) [2] {2}
	763	**25**	**2**	o C5Me wag (8+) [2] {1}	33	397	19	2	o Ri def 3 (57−) [24] {2}
				o N3H wag (7+) [21] {0}		**391(RA)**	**2**		o Ri def 1 (20−) [−15] {1}
				o Ri def 1 (6−) [−33] {0}					o C4O wag (12+) [−6] {0}
				o Me ro (3−) [1] {0}					o N1H wag (9+) [21] {1}
				o Ri def 3 (3−) [7] {0}	34	387	20	1	C2O be (37+) [10] {1}
				o C6H wag (0−) [−4] {0}		**407(RA)**	*c*		C4O be (27−) [9] {1}
				o Ri def 2 (−7−) [2] {1}					N3C4 s (10−) [−1] {0}
				Total (100) [22] {***1***}	35	300	0	0	o C5Me wag (79-) [0] {0}
26[g]	749	52	0	o C2O wag (101−)[68]{0}		**307(RA)**	*c*	**0.6**	o Ri def 1 (18-) [0] {0}
	754	**30**	**0**	o N3H wag (9+) [38] {0}	36	278	3	0	C5Me be (72-) [1] {0}
				o N1H wag (2+) [28] {0}		**282(RA)**	*c*	**0.5**	C4O be (10+) [2] {0}
				o Ri def 1 (−5+) [-47] {0}	37	154	1	0	o Ri def 1 (47-) [2] {0}
				o Ri def 3 (−6−) [−32] {0}		**155(RA)**	*c*	**0.1**	o Ri def 2 (38+) [0] {0}
				Total (101) [55] {***0***}					o Ri def 3 (14+) [2] {0}
27[g]	737	4	13	C4C5 s (39−) [2] {4}	38	139	0	0	Me tor (84-) [0] {0}
	727	**5**	**12**	C5Me s (15−) [0] {1}		**139(RA)**	*c*	**0.1**	
				Ri def 3 (13−) [2] {−1}	39	111	0	0	o Ri def 2 (54+) [0] {0}
				N3C4 s (7−) [0] {2}		*c*	*c*	*c*	o Ri def 3 (43-) [0] {0}

[a] For discussion of the scaling factors for the force constants, see text. [b] (IR) or (RA) next to the frequency indicates that the band is observed only in the IR or RA spectrum. [c] Not possible to measure; the instrumental sensitivity is too small in this region. [d] The total relative intensity for all of the subbands observed for this mode (see Figure 2 and text). [e] Reference for the relative RASS values. See text. [f] All of the values for PEDs, IDs, and RIDs truncated at the 10% level, except for selected normal modes. [g] For these selected modes, all PEDs, IDs, and RIDs greater than 1 are shown. The total sum of PEDs is shown equal to 100% (within rounding error); the sum of IDs is equal to A_c and the sum of RIDs is equal to $RASS_c$, also within the rounding errors. [h] The experimental values for the IR intensity, $\mathbf{A_{exp}}$, and Raman scattering strengths, $\mathbf{RASS_{exp}}$ are *relative* values, as discussed in the text. The assignment of the experimental spectrum is made using this comparison and lists here the calculated contributions to the potential energy, PED in percent, to the infrared intensity, ID in km mol^{-1}, and to the Raman scattering strength, RID in Å^4 amu^{-1}, from each internal coordinate for each normal mode.

In contrast, the internal coordinates that are strongly affected by the hydrogen bonding have large contributions to the infrared intensity. Thus, the infrared spectrum of the solid thymine is very different from that for the isolated molecules. The effect of hydrogen bonding on the IR and RA spectra of thymine and other nucleic-acid bases will be the subject of further theoretical and experimental study in forthcoming publications.

Concluding Remarks

Probably the most important conclusion from this study is its strong reinforcement of the old adage that it is useful to measure experimentally *both* IR *and* RA spectra before trying to make a definitive assignment of the vibrational spectrum of a molecule, especially one that is as complex as thymine. We

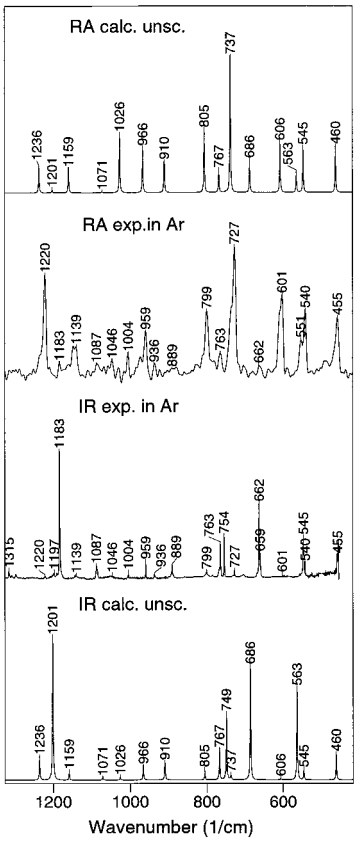

Figure 6. Comparison of the experimental Raman and infrared spectra in the 1320−400 cm^{-1} spectral region, of thymine isolated in an Ar matrix at about 12 K, with the unscaled spectra from the B3LYP/6-31G(d,p) calculation. The vertical scale is described in Figure 1.

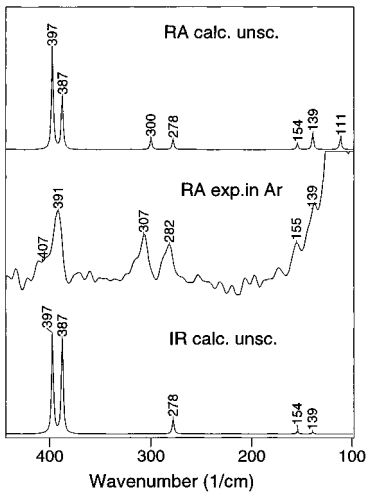

Figure 7. Continuation of the comparison in Figure 6 to the 400−100 cm^{-1} region of the experimental Raman spectrum of thymine isolated in the Ar matrix at 12 K, with the unscaled spectrum from the B3LYP/6-31G(d,p) calculation.

have seen, above, several examples of modes with nearly zero activity in the IR spectrum but relatively strong activity in the RA, and vice versa. Although it may sometimes be possible to make an assignment of the entire vibrational spectrum anyway, especially with the help of a very good quantum-mechanical calculation and a very well-developed chemical intuition, experimental data from both IR and RA spectra allow an assignment to be made with much greater confidence in its validity.

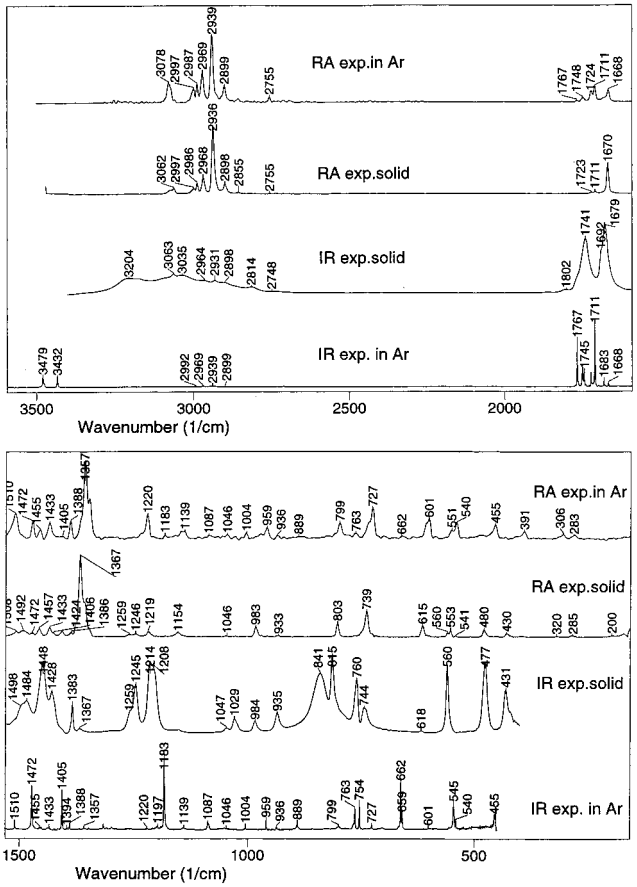

Figure 8. Comparison of the experimental Raman and infrared spectra in the entire spectral region of thymine isolated in an Ar matrix at about 12 K with those for polycrystalline thymine. The vertical scale is described in the caption for Figure 1. The IR spectra were measured on solid thymine at room temperature in a KBr pellet; Raman spectra were measured for a solid sample placed in a small cavity in the aluminum block.

Having said this, we must go on to point out that our assignment here is not basically different from that by Nowak et al.,[4,10,11] which was made without the benefit of the Raman spectrum. We believe that our results confirm their results rather strongly, primarily by the observation in the Raman spectrum of strong bands confirming the reality of corresponding weak absorption features in the IR spectrum that had been assigned as fundamentals. We think that the assignment of the vibrational spectra of isolated thymine is now essentially complete. The assignment of the spectra for solid thymine, which has been the subject of so much work in the past, may be aided by this work, but the intermolecular forces in the solid have a profound effect on the appearance of IR spectrum, such that correspondence between bands observed in the solid and those observed here for the isolated molecule is not obvious. Here, we simply want to offer two tentative conclusions: First, the IR spectrum is more sensitive to hydrogen bonding and is the preferred technique for study of this interaction. Second, the RA spectrum is relatively insensitive to hydrogen bonding, so the RA spectrum of the solid can be successfully interpreted using calculations made for isolated molecules. We expect to make this subject the goal of our next study.

Finally, we conclude that the DFT calculation of vibrational spectra at the B3LYP/6-31G(d,p) level appears to be very good, indeed. On the basis of our experience with calculations of vibrational spectra for a variety of molecules, we can only say that this very high level of agreement is a pleasant contrast with

results from scaled HF/6-31G(d,p) calculations (or even those from MP2/6-31+G(d,p) calculations), which we have used previously. We believe that there are still some errors in the predicted values of harmonic frequencies (on the order of 1−3% in frequency, suggesting something on the order of 2−6% for force constants). It is probable that similar errors are present in the predicted intensity parameters (dipole derivatives and polarizability derivatives), leading to somewhat larger errors in the calculated absolute absorption coefficients or scattering strengths. Nevertheless, the errors in both frequencies and intensities due to anharmonicity and to necessary corrections to experimental values are now nearly as, or perhaps even more, important as are the potential errors in the calculations alone. The major problem remaining involves the necessity of accurate calculation of force constants that control the mixing of internal coordinates and then accounting for the anharmonicity of the experimental spectra.

Acknowledgment. It means a great deal to us that we are able to dedicate this contribution to Marilyn Jacox in acknowledgment of her leadership in this field, her inspiration and encouragement of our own work, and especially for her valued friendship over the years. We are also grateful to NIH (Grant No. 32988) for their small but crucial financial support of the early stage of this work and to NSF for a grant involving the purchase of the Raman spectrometer. We appreciate the preliminary frequency and IR intensity results from DFT calculations made several years ago by Janet E. Del Bene, which encouraged us to re-do the calculation and extend it to include the Raman spectrum.

References and Notes

(1) Jacox, M. E. Vibrational and Electronic Energy Levels of Polyatomic Transient Molecules. *J. Phys. Chem. Ref. Data* **1994**, No.3, A. C. S, A. I. P.; N.S. R. D. S., and references therein.

(2) Person, W. B.; Szczepaniak, K.; Szczesniak, M. M.; Del Bene, J. E. In *Recent Experimental and Computational Advances in Molecular Spectroscopy*; Fausto R., Ed.; NATO ASI Series; Kluwer: Dordrecht, 1993; pp 141−169.

(3) Person, W. B.; Szczepaniak, K. In *Vibrational Spectra and Structure*; Durig, J. R., Ed.; Elsevier: Amsterdam, 1993, Vol. 20, p 239.

(4) Nowak, M. J.; Lapinski, L.; Kwiatkowski, J. S.; Leszczynski, J. *Comput. Chem. Rev.* **1997**, *2*, 140.

(5) Barnes, A. J.; Stuckey, M. A.; LeGall, L. *Spectrochim. Acta, Part A* **1984**, *40A*, 419.

(6) Aida, M.; Kaneko, M.; Dupuis, M.; Ueda, T.; Ushizawa, K.; Ito, G.; Kumakura, A.; Tsuboi, M. *Spectrochim. Acta, Part A* **1997**, *53A*, 393.

(7) Tsuboi, M.; Kumakura, A.; Aida, M.; Kaneko, M.; Dupuis, M.; Ushizawa, K.; Ueda, T. *Spectrochim. Acta, Part A* **1997**, *53A*, 409.

(8) Rush, T., III.; Peticolas, W. L. *J. Phys. Chem.* **1995**, *99*, 14 647.

(9) Aamouche, A.; Ghomi, M.; Grajcar, L.; Baron, M. H.; Jobic, H.; Berthier, G. *J. Phys. Chem. A* **1997**, *101*, 1808.

(10) Nowak, M. J. *J. Mol. Struct.* **1989**, *193*, 35.

(11) Les, A.; Adamowicz, L.; Nowak, M. J.; Lapinski, L. *Spectrochim. Acta, Part A* **1992**, *48A*, 1385.

(12) Graindourze, M.; Smets, J.; Zeegers-Huyskens, Th.; Maes, G. *J. Mol. Struct.* **1990**, *222*, 345.

(13) *GRAMS/32*, Galactic Industries Corp., 1996.

(14) *SPECTRACALC*, Galactic Industries Corp., 1990.

(15) *The Merck Index, 11th ed.*; Merck & Co., Inc.: Rahway, New Jersey, 1989; p 9332.

(16) Hendra, P.; Jones, C.; Warnes, G. *Fourier Transform Raman Spectroscopy. Instrumentation and Chemical Applications*; Ellis Horwood: New York, 1991; Chapter 6.

(17) Placzek, G. In *Handbuch der Radiologie*; Marx, E., Ed.; Akademische Verlagsgesellschaft M. B. H.: Leipzig, 1934; Part II, Vol. 6, p 205.

(18) Frisch, M. J.; Trucks, G. W.; Schlegel, H. B.; Scuseria, G. E.; Robb, M. A.; Cheeseman, J. R.; Zakrzewski, V. G.; Montgomery, J. A., Jr.; Stratmann, R. E.; Burant, J. C.; Dapprich, S.; Millam, J. M.; Daniels, A. D.; Kudin, K. N.; Strain, M. C.; Farkas, O.; Tomasi, J.; Barone, V.; Cossi, M.; Cammi, R.; Mennucci, B.; Pomelli, C.; Adamo, C.; Clifford, S.; Ochterski, J.; Petersson, G. A.; Ayala, P. Y.; Cui, Q.; Morokuma, K.; Malick, D. K.; Rabuck, A. D.; Raghavachari, K.; Foresman, J. B.; Cioslowski, J.; Ortiz, J. V.; Stefanov, B. B.; Liu, G.; Liashenko, A.; Piskorz, P.; Komaromi, I.; Gomperts, R.; Martin, R. L.; Fox, D. J.; Keith, T.; Al-Laham, M. A.; Peng, C. Y.; Nanayakkara, A.; Gonzalez, C.; Challacombe, M.; Gill, P. M. W.; Johnson, B.; Chen, W.; Wong, M. W.; Andres, J. L.; Gonzalez, C.; Head-Gordon, M.; Replogle, E. S.; Pople, J. A. *GAUSSIAN 98, Revision A.3;* GAUSSIAN Inc.: Pittsburgh, PA, 1998.

(19) Parr, R. G.; Yang, W. *Density Functional Theory of Atoms and Molecules*; Oxford University Press: New York, 1989.

(20) Labanowski, J. K.; Anzelm, W. J. *Density Functional Methods in Chemistry*; Springer-Verlag: New York, 1991.

(21) Becke, A. D. *J. Chem. Phys.* **1993**, *98*, 5648.

(22) (a) Chin, S. *program PACK*; written based on *program CHARLY* from Overend, J. *Program Manual of the Molecular Spectroscopy Laboratory*, University of Minnesota, 1966. (b) KuBulat, K.; Person, W. B. *program PACK95*, based on *PACK*; see KuBulat, K. Ph.D. dissertation, University of Florida, 1989. (c) Chabrier, P.; Person, W. B. *program XTRAPACK*, based on (a) and (b); see Chabrier, P. Ph.D. dissertation, University of Florida, 1998.

(23) Califano, S. *Vibrational States*; Wiley: London, 1976.

(24) For example, see: Hedberg, L.; Mills, I. *J. Mol. Spectrosc.* **1993**, *160*, 117. Mills, I. In *Recent Experimental and Computational Advances in Molecular Spectroscopy;* NATO ASI Series; Fausto, R., Ed.; Kluwer: Dordrecht, 1993; pp 79−98.

(25) Morino, Y.; Kuchitso, K. *J. Chem. Phys.* **1952**, *20*, 1809.

(26) Qian, W.; Krimm, S. *J. Phys. Chem.* **1993**, *97*, 11 578.

(27) *ANIMOL 3.2., Infrared and Raman Spectroscopy Teaching and Research Tool for Windows*; Innovative Software: Gainesville, FL, 1996.

(28) Murphy, W. F.; Zerbetto, F.; Duncan, J. L.; McKean, D. C. *J. Phys. Chem.* **1993**, *97*, 581.

(29) Law, M. M.; Duncan, J. L. *Mol. Phys.* **1998**, *93*, 809.

(30) Rosenstock, M.; Rosmus, P.; Reinsch, E.-A.; Treutler, O.; Carter, S.; Handy, N. C. *Mol. Phys.* **1998**, *93*, 853.

(31) Law, M. M.; Duncan, J. L. *Mol. Phys.* **1991**, *74*, 861.

(32) Szczepaniak, K. unpublished results from studies of fundamental and overtone frequencies of the C═O stretching modes of solid 1,3-dimethyluracil, which indicate an anharmonicity correction of about 60−70 cm^{-1} for the C═O stretch, and of the NH stretch for pyrrole in CCl_4 solution, which indicate an anharmonicity correction of 140−150 cm^{-1} for the NH stretch.

(33) Herzberg, G. *Molecular Spectra and Molecular Structure. I. Spectra of Diatomic Molecules*, 2nd ed.; Van Nostrand: New York, 1950.

(34) Szczesniak, M.; Nowak, M. J.; Rostkowska, H.; Szczepaniak, K.; Person, W. B. *J. Am. Chem. Soc.* **1983**, *105*, 5969.

(35) Szczepaniak, K.; Person, W. B.; Leszczynski, J.; Kwiatkowski, J. S. *Pol. J. Chem.* **1998**, *72*, 402.